Digital Signal Processing ••• (••••) •••–•••

Contents lists available at ScienceDirect

Digital Signal Processing

www.elsevier.com/locate/dsp

Quaternion-MUSIC for near-field strictly noncircular sources with large-scale polarization array

Weifeng Wang [a], Hua Chen [b,*], Jie Jin [a], Xianpeng Wang [c], Liangtian Wan [d], Xiaowei Zhang [b]

[a] School of Electronic Information Engineering, Tianjin University, Tianjin 300072, China
[b] Faculty of Information Science and Engineering, Ningbo University, Ningbo 315211, China
[c] State Key Laboratory of Marine Resource Utilization in South China Sea, College of Information Science and Technology, Hainan University, Haikou 570228, China
[d] Key Laboratory for Ubiquitous Network and Service Software of Liaoning Province, School of Software, Dalian University of Technology, Dalian 116620, China

ARTICLE INFO

Article history:
Available online xxxx

Keywords:
DOA estimation
Near-field
Noncircular signals
Quaternion
Massive MIMO

ABSTRACT

In this paper, a novel localization method is proposed for DOA, range and polarization estimation of near-field noncircular sources in massive multiple-input-multiple-output (MIMO) systems. Compared with traditional MUSIC-based algorithms, the proposed algorithms can separate the polarization parameters from the spatial spectrum function, avoiding the four-dimensional (4-D) spectrum search and realizing the fast localization of the near-field source with high accuracy. First, the dimension-reduced MUSIC (DR-MUSIC) algorithm is proposed for DOA and range estimation with low computational complexity, and given a closed-form expression of polarization estimation. Next, based on the quaternion theory, a novel algorithm named quaternion non-circular MUSIC (QNC-MUSIC) is proposed for parameter estimation of non-circular signals with high estimation accuracy. In addition, the analysis of the computational complexity and simulations of the proposed method are provided, showing that the proposed method yields a better performance than DR-MUSIC in massive MIMO systems.

1. Introduction

Massive multiple-input-multiple-output (MIMO), where a base station (BS) equipped with a large number of antennas, is the key enabling technology for gigabit-per-second data transmission in the next generation wireless communication system [1,2]. With the spatial freedom offered by large antenna arrays, abundant mobile terminals are expected to occupy the same set of time and frequency resources with negligible interference [3], and the network capacity and transmission efficiency of the system can be greatly improved.

Attracted by the promising properties of the massive MIMO technique, extensive research such as interference mitigation [4], multiuser beamforming [5] has been conducted both on theoretical studies and practical implementations. However, channel modeling, one of the important tools to evaluate the performance of massive MIMO systems is required in all above researches and Direction-of-arrivals (DOAs) of signal paths, as the crucial parameters of channel physical model, its estimation precision directly determines the quality of the channel model. Thus, accurate DOA estimation is a prerequisite for channel modeling in massive MIMO systems.

The traditional DOA estimation algorithms, such as MUSIC [6] and ESPRIT [7], follow a hypothesis that the distance from the sources to the array is infinity. However, with the increase of the number of antennas in massive MIMO systems, the array size increases sharply which contributes to a large Rayleigh distance [8]. At this time, the far-field hypothesis is no longer satisfied. The traditional algorithms of estimating far-field sources cannot be directly used to estimate near-field sources, therefore it is important to develop localization methods for near-field sources in massive MIMO systems.

Recent researches have shown that the performance improvement of DOA estimation methods can be attained by using the polarization sensitive array and coprime array in wireless communication applications [9–12]. As far as the near-field source localization problem is concerned, the least squares-virtual ESPRIT algorithm based on fourth-order statistics (FOS) has been proposed in [13]. Following the higher order statistics (HOS) idea, He et al. [14] proposed the maximum likelihood method and subspace-based method for partially polarized sources. In order to reduce the computational complexity and improve the estimation accuracy, some efforts have been made to maintain the vector nature of the po-

* Corresponding author.
E-mail addresses: weifeng_17@tju.edu.cn (W. Wang), dkchenhua0714@hotmail.com (H. Chen), jinjie@tju.edu.cn (J. Jin), wxpeng2016@hainu.edu.cn (X. Wang), wanliangtian@dlut.edu.cn (L. Wan), zhangxiaowei@nbu.edu.cn (X. Zhang).

https://doi.org/10.1016/j.dsp.2019.06.005
1051-2004/

larization sensitive array output within a hyper complex algebra framework [15–17]. In [15], the quaternion-MUSIC (Q-MUSIC) algorithm was proposed, and the collection of a two-component vector-sensor array is represented by a quaternion model, which has higher accuracy in direction finding than traditional MUSIC one. In [17], a quaternion ESPRIT algorithm was proposed for DOA estimation with a crossed-dipole array, and it was shown to outperform the conventional complex ESPRIT algorithm. Therefore, utilizing hyper complex algebra properly can improve the estimation performance.

However, none of these above-mentioned algorithms has considered that the impinging signals are non-circular which have been widely used in modern wireless communication systems, such as QAM and BPSK signals. Recent researches [18,19] have shown that the estimation accuracy can be improved through exploiting the covariance matrix and the pseudo covariance matrix properly. For DOA estimation of non-circular signals, the classical algorithm non-circular multiple signal classification (NC-MUSIC) was proposed in [20], which expanded the array virtual aperture and improved estimation accuracy. Following the idea of expanding the array virtual aperture, Zhou et al. proposed a series of efficient algorithms for virtual array such as coprime array, in [21–23], which improved the robustness and efficiency of the estimation. However, these methods assume that the incoming signals are far-field sources, however, in some practical applications, both near-field and far-field should be considered. Thus a lot of research on the localization of near-field and mixed sources exploiting the non-circular information was reported in [24–27]. In [24], Chen et al. proposed the rank reduction localization method for mixed near-field and far-field rectilinear sources. Furthermore, for DOA estimation of mixed circular and non-circular signals, Chen et al. proposed two two-dimensional direction finding algorithms in [26, 27]. To the best of our knowledge, no contributions have dealt yet with DOA, range and polarization for near-field non-circular signals. Therefore, in this paper, based on a uniform linear polarization array, we proposed a localization method for near-field non-circular sources by exploiting both the non-circular and polarization information of the signals.

Notations: in this paper, $(\cdot)^*$, $(\cdot)^T$, $(\cdot)^H$, $(\cdot)^{-1}$ and $E[\cdot]$ represent operations of conjugation, transpose, conjugate transpose, inverse and expectation respectively. $\mathbb{R}, \mathbb{C}$ and $\mathbb{H}$ represent the number fields of real number, complex number and the quaternion number, respectively. The symbol $diag\{\cdot\}$ stands for the diagonalization operation and $\mathbf{I}_M$ stands for a $M \times M$ identity matrix. $\|\cdot\|_F$ denotes the Frobenius norm. $\arg(\cdot)$ is the phase operator of complex numbers and $det(\cdot)$ is the determinant operator of square matrices. $\otimes$ and $\odot$ are the Kronecker product and Hadamard product operations, respectively.

2. Definition of quaternion and relevant arithmetic

Quaternions are a special hyper complex numbers system, first proposed by Hamilton [28]. Quaternions can be regarded as an extension of complex numbers to four-dimensional (4D) space. Basic properties and more complete material about quaternions can be found in [29,30]. Several basic definitions, notations and properties which would be used in this paper are introduced as follows.

Definition 1. A quaternion has four components (one real part and three imaginary parts) and can be expressed in Cartesian form as

$$\begin{aligned} q &= a + bi + cj + dk \\ &= (a + bi) + (c + di)j \\ &= \alpha + \beta j \end{aligned} \tag{1}$$

where $a, b, c, d \in \mathbb{R}$ are real numbers, $\alpha, \beta \in \mathbb{C}$ are complex number, and i, j, k are imaginary units which obey the following multiplication rules

$$\begin{aligned} ij &= -ji = k, \qquad jk = -kj = i \\ ki &= -ik = j, \qquad i^2 = j^2 = k^2 = -1 \end{aligned} \tag{2}$$

Property 1. The multiplication of two imaginary units is not commutative which means that given two quaternions $q_1, q_2 \in \mathbb{H}$, we have $q_1 q_2 \neq q_2 q_1$.

Definition 2. The notation q^* which represents the conjugate of quaternion q, is defined as

$$q^* = a - bi - cj - dk \tag{3}$$

Property 2. Given two quaternions $q_1, q_2 \in \mathbb{H}$, we have $(q_1 q_2)^* = q_2^* q_1^*$ and for a complex number $\alpha \in \mathbb{C}$, we have $\alpha j = j\alpha^*$.

Definition 3. The matrix $\mathbf{B}$ which is consisted of quaternions called the quaternion matrix, noted with $\mathbf{B} \in \mathbb{H}$.

Property 3. For two quaternion matrix $\mathbf{B} \in \mathbb{H}^{P \times Q}$ and $\mathbf{C} \in \mathbb{H}^{Q \times P}$, we have $(\mathbf{BC})^H = \mathbf{C}^H \mathbf{B}^H$, and for a complex matrix $\mathbf{D} \in \mathbb{C}$, we have $\mathbf{D}j = j\mathbf{D}^*$. It should be noted that, because of $q_1 q_2 \neq q_2 q_1$, in general, we have $(\mathbf{BC})^T \neq \mathbf{C}^T \mathbf{B}^T$.

Definition 4. Given a quaternion matrix $\mathbf{B} \in \mathbb{H}$ it can be expressed as $\mathbf{B} = \mathbf{B}_1 + j\mathbf{B}_2$, with $\mathbf{B}_1, \mathbf{B}_2 \in \mathbb{C}$, by using the Cayley-Dickson notation. Then one can define the complex adjoint matrix [31], corresponding to the quaternion matrix as follows

$$\mathbf{B}^\sigma = \begin{bmatrix} \mathbf{B}_1 & \mathbf{B}_2^* \\ -\mathbf{B}_2 & \mathbf{B}_1^* \end{bmatrix} \tag{4}$$

Property 4. The complex adjoint matrix $\mathbf{B}^\sigma$ is normal, hermitian or unitary if and only if the quaternion matrix $\mathbf{B}$ is normal, hermitian or unitary, and the rank of $\mathbf{B}$ is r if and only if the rank of $\mathbf{B}^\sigma$ is $2r$.

Theorem 1. *A quaternion square matrix $\boldsymbol{B} \in \mathbb{H}^{P \times P}$ which satisfies $\boldsymbol{B} = \boldsymbol{B}^H$ is called self-conjugated matrix. The left and right eigenvalues of self-conjugated matrix $\boldsymbol{B}$ are both real numbers and equal. Moreover, they are the eigenvalues of the complex adjoint matrix $\boldsymbol{B}^\sigma$ as well. This proof can be found in [31].*

For a self-conjugated matrix $\boldsymbol{B} \in \mathbb{H}^{P \times P}$, which can be written as $\boldsymbol{B} = \boldsymbol{B}_1 + j\boldsymbol{B}_2$, with $\boldsymbol{B}_1 = \boldsymbol{B}_1^H$, $\boldsymbol{B}_2 = -\boldsymbol{B}_2^T$. Therefore according to (4), it is known that the complex adjoint matrix $\boldsymbol{B}^\sigma$ is a complex hermite matrix with $2P \times 2P$ dimension. And the EVD of the complex adjoint matrix $\boldsymbol{B}^\sigma$ which can be expressed as

$$\boldsymbol{B}^\sigma = \begin{bmatrix} \boldsymbol{U}_1 & \boldsymbol{U}_2^* \\ -\boldsymbol{U}_2 & \boldsymbol{U}_1^* \end{bmatrix} \begin{bmatrix} \boldsymbol{\Sigma}_P & \mathbf{0} \\ \mathbf{0} & \boldsymbol{\Sigma}_P \end{bmatrix} \begin{bmatrix} \boldsymbol{U}_1 & \boldsymbol{U}_2^* \\ -\boldsymbol{U}_2 & \boldsymbol{U}_1^* \end{bmatrix}^H \tag{5}$$

Where $\boldsymbol{\Sigma}_P = diag(\lambda_1, \lambda_2, \cdots, \lambda_P)$ and the entries on its main diagonal are the eigenvalues of self-conjugated matrix $\boldsymbol{B}$. The special structure of $\boldsymbol{B}^\sigma$ induces the structure in $\boldsymbol{U}_1$ and $\boldsymbol{U}_2$ which represent quaternion vectors in their complex notations. Then the EVD of the quaternion matrix $\boldsymbol{B}$ can be expressed as

$$\boldsymbol{B}^\sigma = \boldsymbol{U}\boldsymbol{\Sigma}_P\boldsymbol{U}^H = (\boldsymbol{U}_1 + j\boldsymbol{U}_2)\boldsymbol{\Sigma}_P(\boldsymbol{U}_1 + j\boldsymbol{U}_2)^H \tag{6}$$

Please cite this article in press as: W. Wang et al., Quaternion-MUSIC for near-field strictly noncircular sources with large-scale polarization array, Digit. Signal Process. (2019), https://doi.org/10.1016/j.dsp.2019.06.005

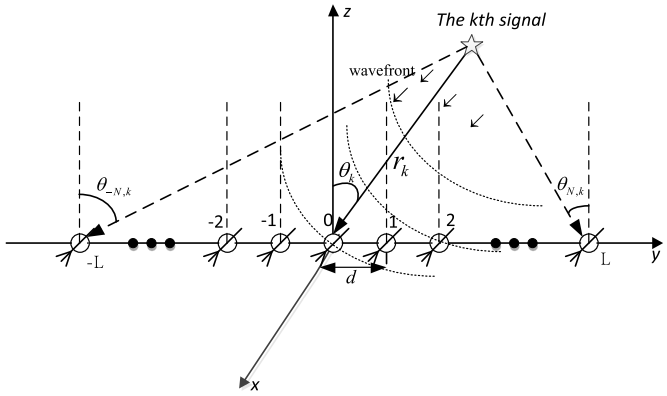

Fig. 1. Array geometry of the ULA considered.

3. Signal and array models

As shown in Fig. 1, consider a uniform linear array (ULA) of $2L+1$ elements, each equipped with concentered orthogonal loop and dipole (COLD). There are K narrowband completely polarized signals located in Fresnel-region of the array. Without loss of generality, we assume the kth near field source in the y_z plane is impinging on the array form the angle $\theta_k \in (-\frac{\pi}{2}, \frac{\pi}{2})$ and range r_k, where the θ_k represents the angle between the kth source and the $z$axis and the r_k denotes the range from the source to the origin of coordinates. The distance of two elements is d, with $d \leq 0.5\lambda_{min}$, where λ_{min} refers to the minimal signals wavelength of the incident signals. The range d which assumed to be within a half-wavelength is to avoid estimation ambiguity.

Let the array center indexed by 0 be the phase reference point. Then the response of the lth $(l = -L, \cdots, 0, \cdots, L)$ sensor corresponding to the angle θ_k, the range r_k of the kth $(k = 1, \cdots, k, \cdots, K)$ source can be modeled as $a(\theta_k, r_k)$ and it is defined as

$$\begin{aligned} a_{lk}(\theta_k, r_k) &= exp(iw_{lk}) \\ &= exp(i\frac{2\pi r_k}{\lambda}(\sqrt{1+(\frac{ld}{r_k})^2 - \frac{2\pi d \sin\theta_k}{r_k}} - 1)) \end{aligned} \tag{7}$$

Where the w_{lk} is the phase offset between the 0th and lth sensors associated with the kth source. For the near-field incident signals, w_{lk} can be expressed as $w_{lk} \approx l\mu_k + l^2\varphi_k$ with second-order expansion, where $\mu_k = -\frac{2\pi d \sin\theta_k}{\lambda}$ and $\varphi_k = \frac{\pi d^2 \cos^2\theta_k}{\lambda r_k}$ are called electric angles. It should be noted that the range of the near-field signal is within the Fresnel region [32]. Although the approximate form of w_{lk} can simplify the expression of (7), it also introduces errors inevitably. Therefore, the exact form of w_{lk} is used in the proposed algorithms.

The completely polarized signals can be decomposed into electric component and magnetic component. An element equipped with orthogonal magnetic loop and dipole measures each polarization component separately, the loop measuring the magnetic component, and the dipole measuring the electric component. For the kth signal, the components of the electromagnetic wave received by the array can be defined as [33]

$$\boldsymbol{\xi}_k = \begin{bmatrix} \xi_{1k} \\ \xi_{2k} \end{bmatrix} = \begin{bmatrix} -\cos\gamma_k \\ -\sin\gamma_k e^{i\eta_k} \end{bmatrix} \tag{8}$$

where ξ_{1k} and ξ_{2k} are the polarization electric component and magnetic component of the signals received by a sensor in the x axis. The $\gamma_k \in (0, \frac{\pi}{2})$ and $\eta_k \in (0, 2\pi)$ represent the polarization angle and polarization phase difference respectively. Thus the data received by the lth sensors at time t can be expressed as

$$\begin{aligned} x_{1l}(t) &= \sum_{k=1}^{K} a_{l,k}(\theta_k, r_k)\xi_{1k}s_k(t) + n_{1l}(t) \\ x_{2l}(t) &= \sum_{k=1}^{K} a_{l,k}(\theta_k, r_k)\xi_{2k}s_k(t) + n_{2l}(t) \end{aligned} \tag{9}$$

Where $s_k(t)$ is the complex envelope of the received signal, $n_{1l}(t)$ and $n_{2l}(t)$ are the additive white Gaussian noise which is independent and identically distributed (I.I.D.) with zero mean and uncorrelated with the sources. Let the vector $\boldsymbol{x}_1(t) = [x_{1(-L)}(t), \cdots, x_{10}(t), \cdots, x_{1L}(t)]^T$ represents the data received by all loops and the vector $\boldsymbol{x}_2(t) = [x_{2(-L)}(t), \cdots, x_{20}(t), \cdots, x_{2L}(t)]^T$ represents the data received by all dipoles, then the data vector received by the array can be expressed as

$$\begin{aligned} \boldsymbol{x}_1(t) &= \mathbf{A}\boldsymbol{\Xi}_1\mathbf{S}(t) + \boldsymbol{n}_1(t) \\ \boldsymbol{x}_2(t) &= \mathbf{A}\boldsymbol{\Xi}_2\mathbf{S}(t) + \boldsymbol{n}_2(t) \end{aligned} \tag{10}$$

where $\mathbf{A} = [\boldsymbol{a}_1, \boldsymbol{a}_2, \cdots, \boldsymbol{a}_K] \in \mathbb{C}^{2L+1\times K}$, $\boldsymbol{a}_k = [a_{(-L),k}, \cdots, 1, \cdots, a_{L,k}]^T$ is the array manifold matrix, $\mathbf{S}(t) = [s_1(t), \cdots, s_K(t)]^T$ is the signal vector, $\boldsymbol{\Xi}_m = diag(\xi_{m1}, \cdots, \xi_{mK})$, $(m = 1, 2)$ are two diagonal matrices constructed by the components of the signal and $\boldsymbol{n}_m(t) = [n_{m(-L)}(t), \cdots, n_{m0}(t), \cdots, n_{mL}(t)]^T$, $(m = 1, 2)$ are the noise vectors whose covariance matrix satisfied $E(\boldsymbol{n}_m(t)\boldsymbol{n}_m^H(t)) = 0$ and $E(\boldsymbol{n}_m(t)\boldsymbol{n}_m^T(t)) = 0$ with a total of N snapshots $t_1, \cdots, t_N$, the received data matrix can be expressed as

$$\mathbf{X}_m = \begin{bmatrix} \boldsymbol{x}_m(t_1) & \boldsymbol{x}_m(t_2) & \cdots & \boldsymbol{x}_m(t_N) \end{bmatrix}, (m = 1, 2) \tag{11}$$

The goal of this paper is to estimate the angle θ_k, range r_k and polarization parameters γ_k and η_k of the kth source from the received data matrix $\mathbf{X}_m$.

4. DR-MUSIC algorithm

In this section, we developed the DR-MUSIC algorithm proposed in [34] to estimate the DOA, range and polarization parameters of the near-field sources with an ULA array. Based on (10), we can combine the data matrices received by all loops and dipoles at time t to an extension matrix and it can be expressed as

$$\boldsymbol{x}(t) = \begin{bmatrix} \boldsymbol{x}_1(t) \\ \boldsymbol{x}_2(t) \end{bmatrix} = \begin{bmatrix} \mathbf{A}\boldsymbol{\Xi}_1 \\ \mathbf{A}\boldsymbol{\Xi}_2 \end{bmatrix}\mathbf{S}(t) + \begin{bmatrix} \boldsymbol{n}_1(t) \\ \boldsymbol{n}_2(t) \end{bmatrix} \tag{12}$$

Then the covariance matrix of $\boldsymbol{x}(t)$ is

$$\mathbf{R} = E[\boldsymbol{x}(t)\boldsymbol{x}^H(t)] = \begin{bmatrix} \mathbf{A}\boldsymbol{\Xi}_1 \\ \mathbf{A}\boldsymbol{\Xi}_2 \end{bmatrix}\mathbf{R}_\mathbf{S}\begin{bmatrix} \mathbf{A}\boldsymbol{\Xi}_1 \\ \mathbf{A}\boldsymbol{\Xi}_2 \end{bmatrix}^H + \sigma_n^2 I_{4L+2} \tag{13}$$

Where $\mathbf{R}_\mathbf{S} = E[\mathbf{S}(t)\mathbf{S}^H(t)]$ denotes the signal covariance matrix which can be written as diagonal form and $\mathbf{I}_{4L+2}$ is the unit matrix of $4L+2$ dimensional.

In practical situations, the theoretical array covariance matrices given in (13) is unavailable and it can be estimated as

$$\widehat{\mathbf{R}} = \frac{1}{N}(\mathbf{X}\mathbf{X}^H) \tag{14}$$

Base on the subspace-based algorithms, the eigenvalue decomposition of $\mathbf{R}$ can be written as

$$\mathbf{R} = \mathbf{U}\boldsymbol{\Lambda}\mathbf{U}^H = \mathbf{U}_\mathbf{S}\boldsymbol{\Lambda}_\mathbf{S}\mathbf{U}_\mathbf{S}^H + \boldsymbol{\Lambda}_\mathbf{N}\mathbf{U}_\mathbf{N}\mathbf{U}_\mathbf{N}^H \tag{15}$$

Where the $(4L+2)\times K$ matrix $\mathbf{U}_\mathbf{S}$ consists of the first K columns of matrix $\mathbf{U}$ called the signal subspace and the

Please cite this article in press as: W. Wang et al., Quaternion-MUSIC for near-field strictly noncircular sources with large-scale polarization array, Digit. Signal Process. (2019), https://doi.org/10.1016/j.dsp.2019.06.005

$(4L+2)\times(4L+2-K)$ matrix $\mathbf{U_N}$ consists of the last $4L+2-K$ columns of matrix $\mathbf{U}$ called the noise subspace. The matrix $\mathbf{\Lambda_S} = diag(\lambda_1,\cdots,\lambda_K)$ and $\Lambda_N = diag(\lambda_{K+1},\cdots,\lambda_{4L+2})$ are diagonal matrices, where $\lambda_1 \geq \lambda_2 \geq \cdots \geq \lambda_K > \lambda_{K+1} = \lambda_{4L+2} = \sigma_n^2$ are the eigenvalues of $\mathbf{R}$. Based on the principle of MUSIC algorithm, the noise subspace $\mathbf{U_N}$ is orthogonal to the signal subspace $\mathbf{U_S}$, then it holds that

$$\begin{bmatrix}\mathbf{A\Xi}_1\\ \mathbf{A\Xi}_2\end{bmatrix}^H \mathbf{U_N} = \mathbf{\Xi}_1^H \begin{bmatrix}\mathbf{A}\\ \mathbf{A\Xi}_2\mathbf{\Xi}_1^{-1}\end{bmatrix}^H \mathbf{U_N} = 0 \tag{16}$$

Blocking $\mathbf{U_N}$ into two $(2L+1)\times(4L+2-K)$ matrices $\mathbf{U_{N1}}$, $\mathbf{U_{N2}}$, then we have

$$\begin{bmatrix}\boldsymbol{a}_1 & \boldsymbol{a}_2\frac{\xi_{21}}{\xi_{11}} & \cdots & \boldsymbol{a}_K\frac{\xi_{2K}}{\xi_{1K}}\\ \boldsymbol{a}_1 & \boldsymbol{a}_2\frac{\xi_{22}}{\xi_{12}} & \cdots & \boldsymbol{a}_K\frac{\xi_{2K}}{\xi_{1K}}\end{bmatrix}^H \begin{bmatrix}\mathbf{U_{N1}}\\ \mathbf{U_{N2}}\end{bmatrix} = 0 \tag{17}$$

Base on (8), the complex number $\frac{\xi_{2k}}{\xi_{1k}}$ can be expressed as

$$\frac{\xi_{2k}}{\xi_{1k}} = \tan\gamma_k e^{i\eta_k} \tag{18}$$

The spectrum function $f_{DR}(\theta_k, r_k, \gamma_k, \eta_k)$ can be constructed as follows

$$\begin{aligned} &f_{DR}(\theta_k, r_k, \gamma_k, \eta_k)\\ &= \|\begin{bmatrix}\boldsymbol{a}_k^H & \tan\gamma_k e^{-i\eta_k}\boldsymbol{a}_k^H\end{bmatrix}\begin{bmatrix}\mathbf{U_{N1}}\\ \mathbf{U_{N2}}\end{bmatrix}\|_F^2\\ &= \boldsymbol{a}_k^H\mathbf{U_{N1}}\mathbf{U_{N1}}^H\boldsymbol{a}_k + \tan\gamma_k e^{-i\eta_k}\boldsymbol{a}_k^H\mathbf{U_{N2}}\mathbf{U_{N1}}^H\boldsymbol{a}_k\\ &+ \tan\gamma_k e^{i\eta_k}\boldsymbol{a}_k^H\mathbf{U_{N1}}\mathbf{U_{N2}}^H\boldsymbol{a}_k + \tan^2\gamma_k\boldsymbol{a}_k^H\mathbf{U_{N2}}\mathbf{U_{N2}}^H\boldsymbol{a}_k \end{aligned} \tag{19}$$

By setting that the partial derivative of $f_{DR}(\theta_k, r_k, \gamma_k, \eta_k)$ with respect to $\tan\gamma_k$ and η_k equal to zero, we can obtain from (19) that

$$e^{-i\eta_k}\boldsymbol{a}_k^H\mathbf{U_{N2}}\mathbf{U_{N1}}^H\boldsymbol{a}_k = e^{i\eta_k}\boldsymbol{a}_k^H\mathbf{U_{N1}}\mathbf{U_{N2}}^H\boldsymbol{a}_k = -\tan\gamma_k\boldsymbol{a}_k^H\mathbf{U_{N2}}\mathbf{U_{N2}}^H\boldsymbol{a}_k \tag{20}$$

Base on (20), it is clear that $e^{i\eta_k}\boldsymbol{a}_k^H\mathbf{U_{N1}}\mathbf{U_{N2}}^H\boldsymbol{a}_k$ is a real number and can be written as

$$e^{i\eta_k}\boldsymbol{a}_k^H\mathbf{U_{N1}}\mathbf{U_{N2}}^H\boldsymbol{a}_k = \sqrt{\|\boldsymbol{a}_k^H\mathbf{U_{N1}}\mathbf{U_{N2}}^H\boldsymbol{a}_k\|_F^2} \tag{21}$$

Then $\tan(\gamma_k)$ is given by

$$\tan\gamma_k = -\frac{\|\boldsymbol{a}_k^H\mathbf{U_{N1}}\mathbf{U_{N2}}^H\boldsymbol{a}_k\|_F^2}{\boldsymbol{a}_k^H\mathbf{U_{N2}}\mathbf{U_{N2}}^H\boldsymbol{a}_k} \tag{22}$$

Substituting (20), (21) and (22) to (19), the spectrum function can be simplified as

$$f_{DR}(\theta_k, r_k) = \boldsymbol{a}_k^H\mathbf{U_{N1}}\mathbf{U_{N1}}^H\boldsymbol{a}_k - \frac{\|\boldsymbol{a}_k^H\mathbf{U_{N1}}\mathbf{U_{N2}}^H\boldsymbol{a}_k\|_F^2}{\boldsymbol{a}_k^H\mathbf{U_{N2}}\mathbf{U_{N2}}^H\boldsymbol{a}_k} \tag{23}$$

Now the DOA and range of the sources can be obtained by two-dimensional peak searching.

The polarization parameters (γ_k, η_k) can be estimated after the K estimated DOAs and ranges have been acquired. Base on (18), (21) and (22), we have

$$c_k = \tan\gamma_k e^{i\eta_k} = -\frac{\|\widehat{\boldsymbol{a}}_k^H\mathbf{U_{N1}}\mathbf{U_{N2}}^H\widehat{\boldsymbol{a}}_k\|_F^2}{\widehat{\boldsymbol{a}}_k^H\mathbf{U_{N1}}\mathbf{U_{N2}}^H\widehat{\boldsymbol{a}}_k\widehat{\boldsymbol{a}}_k^H\mathbf{U_{N2}}\mathbf{U_{N2}}^H\widehat{\boldsymbol{a}}_k} \tag{24}$$

Where the steering vector $\widehat{\boldsymbol{a}}_k$ is constructed by $(\widehat{\theta}_k, \widehat{r}_k)$ which has already been estimated from (23). Thus the polarization estimation of the kth signal is expressed as

$$\begin{aligned}\widehat{\gamma}_k &= \arctan(|c_k|)\\ \widehat{\eta}_k &= \arg(c_k)\end{aligned} \tag{25}$$

Based on the method mentioned above, the DOAs, ranges and polarization estimation can be automatically obtained. The pseudo code of the DR-MUSIC is summarized as

1. Estimate covariance matrix $\widehat{\mathbf{R}}$ according to (14);
2. Take the EVD of $\widehat{\mathbf{R}}$ according to (15);
3. Construct the spectrum function $f_{DR}(\theta_k, r_k)$ according to (23);
4. Search (23) to obtain the spectrum extremum $(\theta_k, r_k), k = 1,\cdots,K$;
5. Calculate c_k according to (24);
6. Estimate polarization parameters $(\gamma_k, \eta_k), k = 1,\cdots,K$ according to (25).

5. QNC-MUSIC algorithm

For a non-circular signal $s(t)$, it holds that [35]

$$E[s(t)s(t)] = \mu\exp(i\beta)E[s(t)s^*(t)] \tag{26}$$

In which β is the non-circularity phase, μ is the non-circularity rate with $\mu = 1$ for the maximal non-circularity rated signal (strictly non-circular). For signal vector $\mathbf{S} \in \mathbb{C}^{K\times 1}$ consisting of K independent maximal non-circularity rated signals, its unconjugated covariance matrix is given by

$$\begin{aligned}\boldsymbol{R'_s} &= E[\boldsymbol{S}(t)\boldsymbol{S}^T(t)]\\ &= diag\{\exp(i\beta_1)E[s_1(t)s_1^*(t)],\\ &exp(i\beta_2)E[s_2(t)s_2^*(t)],\cdots,\\ &exp(i\beta_K)E[s_K(t)s_K^*(t)]\} \triangleq \mathbf{\Phi}\boldsymbol{R_s}\end{aligned} \tag{27}$$

Where $\mathbf{\Phi} = diag\{\exp(i\beta_1), exp(i\beta_2),\cdots,exp(i\beta_K)\}$ is a diagonal matrix consisting of their non-circularity phases.

In order to exploit the non-circular information of the incident signals, we define quaternion steering vector $\boldsymbol{x}(t)$, $\boldsymbol{y}(t)$ with the data vector $\boldsymbol{x}_1(t)$, $\boldsymbol{x}_2(t)$ received by the array and its conjugate as follows

$$\begin{aligned}\boldsymbol{x}(t) &= \boldsymbol{x}_1(t) + \boldsymbol{x}_2(t)j\\ \boldsymbol{y}(t) &= \boldsymbol{x}_1^*(t) + \boldsymbol{x}_2^*(t)j\end{aligned} \tag{28}$$

Substituting (10) into (28), we have

$$\begin{aligned}\boldsymbol{x}(t) &= \mathbf{A}(\mathbf{\Xi}_1 + \mathbf{\Xi}_2 j)\mathbf{S}(t) + (\boldsymbol{n}_1(t) + \boldsymbol{n}_2(t)j)\\ &= \mathbf{A\Xi}_x\mathbf{S}(t) + \boldsymbol{n}_x(t)\\ \boldsymbol{y}(t) &= \mathbf{A}^*(\mathbf{\Xi}_1^* + \mathbf{\Xi}_2^* j)\mathbf{S}^*(t) + (\boldsymbol{n}_1^*(t) + \boldsymbol{n}_2^*(t)j)\\ &= \mathbf{A}^*\mathbf{\Xi}_y\mathbf{S}^*(t) + \boldsymbol{n}_y(t)\end{aligned} \tag{29}$$

Where $\mathbf{\Xi}_x \in \mathbb{H}^{K\times K}$ and $\mathbf{\Xi}_y \in \mathbb{H}^{K\times K}$ are diagonal quaternion matrices and the diagonal entries of $\mathbf{\Xi}_x$ and $\mathbf{\Xi}_y$ are $\xi_{xk} = \xi_{1k} + \xi_{2k}j$ and $\xi_{yk} = \xi_{1k}^* + \xi_{2k}^* j$, $k = 1,\cdots,K$

Combine $\boldsymbol{x}(t) \in \mathbb{H}^{2L+1\times K}$ and $\boldsymbol{y}(t) \in \mathbb{H}^{2L+1\times K}$ into a quaternion vector $\boldsymbol{z}(t)$ that be constructed as

$$\boldsymbol{z}(t) = \begin{bmatrix}\boldsymbol{x}(t)\\ \boldsymbol{y}(t)\end{bmatrix} = \begin{bmatrix}\boldsymbol{x}_1(t)\\ \boldsymbol{x}_1^*(t)\end{bmatrix} + \begin{bmatrix}\boldsymbol{x}_2(t)\\ \boldsymbol{x}_2^*(t)\end{bmatrix} j = \boldsymbol{z}_1(t) + \boldsymbol{z}_2(t)j \tag{30}$$

The quaternion covariance matrix $\boldsymbol{R_z} \in \mathbb{H}^{4L+2\times 4L+2}$ is

$$\mathbf{R_z} = E[\boldsymbol{z}(t)\boldsymbol{z}^H(t)] = \begin{bmatrix}E(\boldsymbol{x}(t)\boldsymbol{x}^H(t)) & E(\boldsymbol{x}(t)\boldsymbol{y}^H(t))\\ E(\boldsymbol{y}(t)\boldsymbol{x}^H(t)) & E(\boldsymbol{y}(t)\boldsymbol{y}^H(t))\end{bmatrix} \tag{31}$$

Substituting (27), (29) into (31) and using the non-circular property, we can simplify the quaternion covariance matrix $\boldsymbol{R_z}$ as

Please cite this article in press as: W. Wang et al., Quaternion-MUSIC for near-field strictly noncircular sources with large-scale polarization array, Digit. Signal Process. (2019), https://doi.org/10.1016/j.dsp.2019.06.005

$$\mathbf{R_z} = \begin{bmatrix} \mathbf{A}\Xi_x \\ \mathbf{A}^*\Xi_y\Phi^* \end{bmatrix} \mathbf{R_S} \begin{bmatrix} \mathbf{A}\Xi_x \\ \mathbf{A}^*\Xi_y\Phi^* \end{bmatrix}^H + 2\sigma_n^2\mathbf{I}_{4L+2} \tag{32}$$

Where $\mathbf{\Phi} = diag(e^{i\phi_1,\cdots,e^{i\phi_K}})$ is a diagonal matrix consisting of their non-circular phases $\phi_k, k = 1, \cdots, K$.

In practical situations, we use the maximum likelihood estimation of $\boldsymbol{R_z}$ to replace the theoretical array covariance matrix

$$\begin{aligned} \widehat{\mathbf{R}}_{\boldsymbol{z}} &= \frac{1}{N}(\mathbf{Z}\mathbf{Z}^H) = \frac{1}{N}(\mathbf{Z}_1 + \mathbf{Z}_2 j)(\mathbf{Z}_1 + \mathbf{Z}_2 j)^H \\ &= \mathbf{R}_{\boldsymbol{z1}} + j\mathbf{R}_{\boldsymbol{z2}} \end{aligned} \tag{33}$$

Where $\mathbf{Z} \in \mathbb{H}^{4L+2\times N}$, $\boldsymbol{Z_1} \in \mathbb{C}^{4L+2\times N}$ and $\boldsymbol{Z_2} \in \mathbb{C}^{4L+2\times N}$ are the snapshot data matrices constructed with $\boldsymbol{z}(t)$, $\boldsymbol{z_1}(t)$ and $\boldsymbol{z_2}(t)$, respectively.

Obviously, the covariance matrix $\mathbf{R_z}$ is a quaternion self-conjugated matrix and its complex adjoint matrix $\mathbf{R}_{\boldsymbol{z}}^{\sigma}$ is a complex hermite matrix. According to the complex adjoint matrix defined in (4), we can get the EVD of complex hermite adjoint matrix $\mathbf{R}_{\boldsymbol{z}}^{\sigma}$

$$\mathbf{R}_{\boldsymbol{z}}^{\sigma} = \begin{bmatrix} \mathbf{R_{z1}} & \mathbf{R}_{\boldsymbol{z2}}^* \\ -\mathbf{R_{z2}} & \mathbf{R}_{\boldsymbol{z1}}^* \end{bmatrix} = \begin{bmatrix} \mathbf{U}_1 & \mathbf{U}_2^* \\ -\mathbf{U}_2 & \mathbf{U}_1^* \end{bmatrix} \begin{bmatrix} \mathbf{\Lambda} & \mathbf{0} \\ \mathbf{0} & \mathbf{\Lambda} \end{bmatrix} \begin{bmatrix} \mathbf{U}_1 & \mathbf{U}_2^* \\ -\mathbf{U}_2 & \mathbf{U}_1^* \end{bmatrix}^H \tag{34}$$

According to the EVD of self-conjugated matrix defined in (5) and (6), we perform EVD of matrix covariance matrix $\mathbf{R_z}$ as follows

$$\begin{aligned} \mathbf{R_z} &= \mathbf{U}\mathbf{\Lambda}\mathbf{U}^H \\ &= (\mathbf{U}_1 + j\mathbf{U}_2)\mathbf{\Lambda}(\mathbf{U}_1 + j\mathbf{U}_2)^H \\ &= \mathbf{U_S}\Lambda_{\mathbf{S}}\mathbf{U}_{\mathbf{S}}^H + 2\sigma_n^2\mathbf{U_N}\mathbf{U}_{\mathbf{N}}^H \end{aligned} \tag{35}$$

Based on the orthogonality between the signal subspace $\mathbf{U_S}$ and noise subspace $\mathbf{U_N}$, it holds that

$$\begin{bmatrix} \mathbf{A}\Xi_x \\ \mathbf{A}^*\Xi_y\mathbf{\Phi}^* \end{bmatrix} \mathbf{U_N} = 0 \tag{36}$$

Dividing the noise subspace matrix into two block matrices $\mathbf{U_{N1}}$, $\mathbf{U_{N2}}$, we can construct the spectrum function of QNC-MUSIC as

$$\begin{aligned} &f_{QNC}(\theta_k, r_k, \gamma_k, \eta_k) \\ &= \| \begin{bmatrix} \boldsymbol{a}_k\xi_{xk} \\ \boldsymbol{a}_k^*\xi_{yk}e^{-i\phi_k} \end{bmatrix}^H \begin{bmatrix} \mathbf{U_{N1}} \\ \mathbf{U_{N2}} \end{bmatrix} \|_F^2 \\ &= \begin{bmatrix} \xi_{xk} \\ \xi_{yk}e^{-i\phi_k} \end{bmatrix}^H \begin{bmatrix} \boldsymbol{a}_k^H\mathbf{U_{N1}}\mathbf{U}_{\mathbf{N1}}^H\boldsymbol{a}_k & \boldsymbol{a}_k^H\mathbf{U_{N1}}\mathbf{U}_{\mathbf{N2}}^H\boldsymbol{a}_k^* \\ \boldsymbol{a}_k^T\mathbf{U_{N2}}\mathbf{U}_{\mathbf{N1}}^H\boldsymbol{a}_k & \boldsymbol{a}_k^T\mathbf{U_{N2}}\mathbf{U}_{\mathbf{N2}}^H\boldsymbol{a}_k^* \end{bmatrix} \begin{bmatrix} \xi_{xk} \\ \xi_{yk}e^{-i\phi_k} \end{bmatrix} \\ &= \mathbf{P}^H(\gamma_k, \eta_k, \phi_k)\mathbf{M}(\theta_k, r_k)\mathbf{P}(\gamma_k, \eta_k, \phi_k) \end{aligned} \tag{37}$$

Where $\mathbf{M}(\theta_k, r_k)$ is the function that only contain the DOA and range parameters and in generation, the rank of $\mathbf{P}(\gamma_k, \eta_k, \phi_k)$ is 1, therefore the rank of $f_{QNC}(\theta_k, r_k, \gamma_k, \eta_k)$ and $\mathbf{M}(\theta_k, r_k)$ are equal, which means the spectrum function can be simplified as

$$f_{QNC}(\theta_k, r_k) = det[\mathbf{M}(\theta_k, r_k)] \tag{38}$$

For the polarization estimation, since the DOA and range have been estimated from (38), we can get the polarization parameters by substituting the estimated DOAs and ranges into (24) and (25).

Until now, the DOAs, ranges and polarization estimation can be automatically obtained by the QNC-MUSIC method whose pseudo code can be summarized as

1. Estimate covariance matrices $\widehat{\boldsymbol{R}}_{\boldsymbol{z}}$ according to (33);
2. Construct the complex adjoint matrix $\mathbf{R}_{\boldsymbol{z}}^{\sigma}$ and perform the EVD of it according to (34);
3. Construct the spectrum function $f_{QNC}(\theta_k, r_k)$ according to (38);
4. Search (38) to obtain the spectrum extremum $(\theta_k, r_k), k = 1, \cdots, K$;
5. Estimate covariance matrices $\widehat{\mathbf{R}}$ according to (14);
6. Take the EVD of $\widehat{\mathbf{R}}$ according to (15);
7. Calculate c_k according to (24);
8. Estimate polarization parameters $(\gamma_k, \eta_k), k = 1, \cdots, K$ according to (25).

6. Computational complexity analysis

In this section, we will analyze the computational complexity of the QNC-MUSIC, the DR-MUSIC and the classical LV-MUSIC method from four parts: the estimation of the covariance matrix, the EVD of the covariance matrix, the spectrum search of the DOA and range parameters and the spectrum search of the polarization parameters. To simplify the expression, we use $M = 2L + 1$ to represent the number of elements, K and N to represent the number of signals and the snapshots. Q_1, Q_2, Q_3 and Q_4 are stand for the number of spectral points for parameter θ, r, γ and η, respectively.

For the classical LV-MUSIC, the dimension of the received data matrix is $2M \times N$, thus $4M^2N$ flops are required for the calculation of the covariance matrix. The complexity of performing EVD on the covariance matrix is $4M^3$ flops. For the spectrum search of the DOA, range and polarization parameters, $Q_1Q_2Q_3Q_4(2M)(2M - K)$ flops are needed to compute $\|[\boldsymbol{a}_{LV}^H(\theta, r, \gamma, \eta)\boldsymbol{U_N}]\|_F^2$ for each spectral point, where $\boldsymbol{a}_{LV}(\theta, r, \gamma, \eta) \in \mathbb{C}^{2M\times 1}$ and $\boldsymbol{U_N} \in \mathbb{C}^{2M\times 2M-K}$ are the steering vector and noise subspace belonging to the LV-MUSIC. Therefore, the computational complexity of the LV-MUSIC is $C_{LV} = Q_1Q_2Q_3Q_4(2M)(2M - K) + 4M^2N + 4M^3$.

For DR-MUSIC, the dimension of the received data matrix is identical with that of the LV-MUSIC, thus $4M^2N$ and $4M^3$ flops are required for the calculation of the covariance matrix and the EVD of the covariance matrix. For the spectrum search of the DOA, range parameters, it has to compute $\boldsymbol{a}_{DR}^H\mathbf{U_{N1}}\mathbf{U}_{\mathbf{N1}}^H\boldsymbol{a}_{DR}$, $\boldsymbol{a}_{DR}^H\mathbf{U_{N1}}\mathbf{U}_{\mathbf{N2}}^H\boldsymbol{a}_{DR}$ and $\boldsymbol{a}_{DR}^H\mathbf{U_{N2}}\mathbf{U}_{\mathbf{N2}}^H\boldsymbol{a}_{DR}$ where $\boldsymbol{a}_{DR} \in \mathbb{C}^{M\times 1}$ and $\boldsymbol{U_{N1}}, \boldsymbol{U_{N2}} \in \mathbb{C}^{M\times 2M-K}$ according to (23) for each spectral point. Therefore, the spectral search step cost $3Q_1Q_2(M)(2M - K)$ flops. According to (24), it can be seen that an analytical solution is given for the polarization parameters, the spectrum search is not needed. Therefore, the computational complexity of the DR-MUSIC is $C_{DR} = 3Q_1Q_2(M)(2M - K) + 4M^2N + 4M^3$.

For QNC-MUSIC, the complex adjoint matrix of the quaternion covariance matrix in (33), require $4M^2N$ flops to be calculated, and the computational complexity of the EVD of the complex adjoint matrix is $16M^3$ flops. For the spectrum search of the DOA and range parameters, it has to compote $\boldsymbol{a}_{QNC}^H\mathbf{U_{N1}}\mathbf{U}_{\mathbf{N1}}^H\boldsymbol{a}_{QNC}$, $\boldsymbol{a}_{QNC}^H\mathbf{U_{N1}}\mathbf{U}_{\mathbf{N2}}^H\boldsymbol{a}_{QNC}^*$ and $\boldsymbol{a}_{QNC}^T\mathbf{U_{N2}}\mathbf{U}_{\mathbf{N2}}^H\boldsymbol{a}_{QNC}^*$ where $\boldsymbol{a}_{QNC} \in \mathbb{H}^{M\times 1}$ and $\boldsymbol{U_{N1}}, \boldsymbol{U_{N2}} \in \mathbb{H}^{M\times 2M-K}$ according to (23) for each spectral point, the spectral search step costs $6Q_1Q_2(M)(2M - K)$ flops. For the polarization parameters, the EVD of (15) has to be taken, the spectrum search is not needed. Therefore, the computational complexity of the QNC-MUSIC is $C_{QNC} = 6Q_1Q_2(M)(2M - K) + 8M^2N + 20M^3$.

Obviously, in terms of implementation, the LV-MUSIC algorithm is significantly more complicated than that of the QNC-MUSIC and the DR-MUSIC algorithms in the context of the massive MIMO systems.

7. Simulation results

In this section, three computer simulations are conducted to demonstrate the performance of the proposed methods (QNC-MUSIC, DR-MUSIC) as compared with QDR method in [36] and the deterministic CRB which was derived from the accurate near-field noncircular signal model in [37–39]. The classical LV-MUSIC is not considered in our simulations because of its prohibitive

Please cite this article in press as: W. Wang et al., Quaternion-MUSIC for near-field strictly noncircular sources with large-scale polarization array, Digit. Signal Process. (2019), https://doi.org/10.1016/j.dsp.2019.06.005

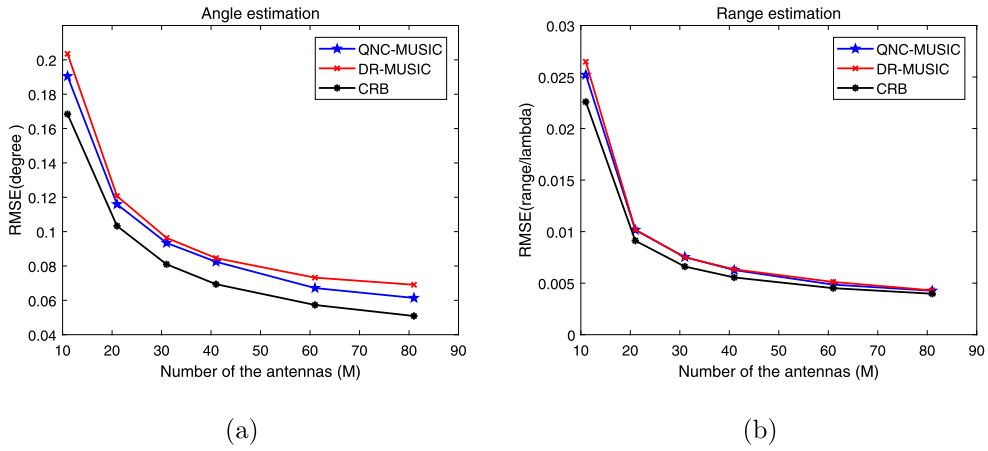

Fig. 2. RMSEs versus the number of the antennas M for the estimates of DOA and range parameters, and the SNR is $0dB$ the snapshot is 200. (a) DOA estimation. (b) Range estimation.

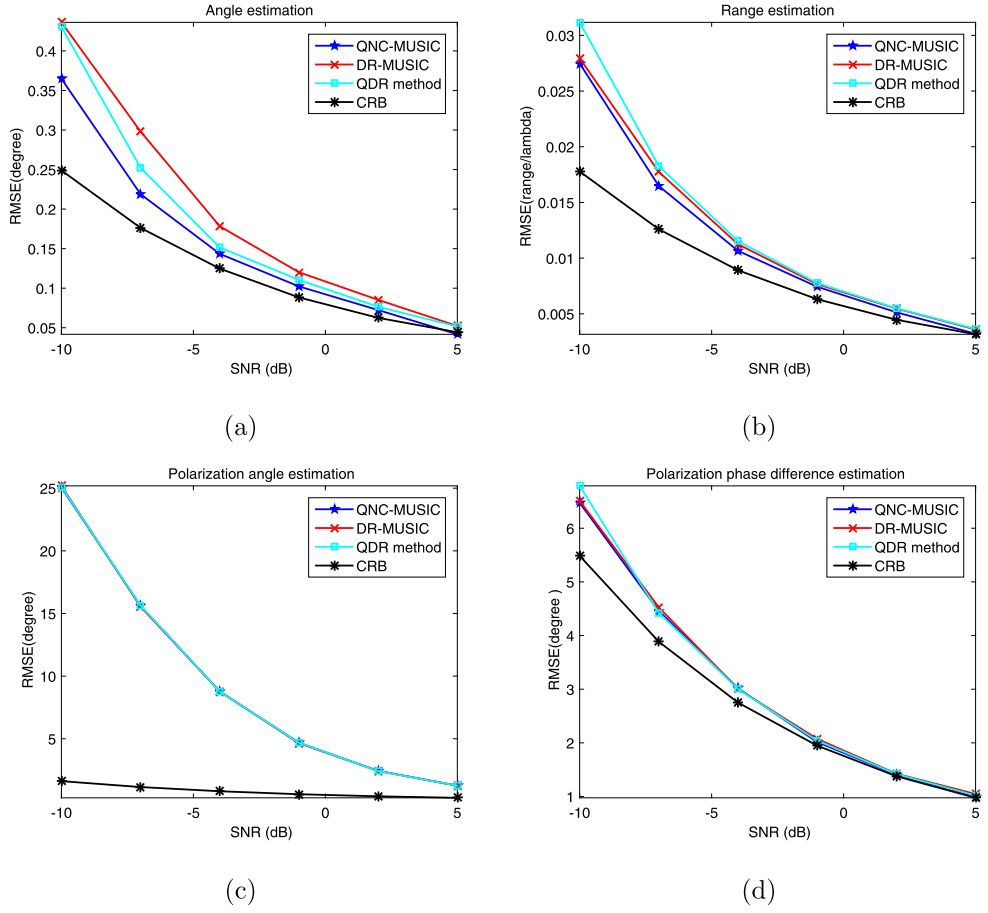

Fig. 3. RMSEs versus SNR with snapshot to be 100. (a) angle estimation. (b) range estimation. (c) polarization angle estimation. (d) polarization phase difference estimation.

computational complexity. In the three simulations, we consider a ULA equipped with COLDs shown in Fig. 1, the distance of two COLDs is set to be 0.5λ. The impinging sources are unit power, uncorrelated BPSK signals, and the additive noise is assumed to be additive white Gaussian noise. The search step size 0.1° and 0.01 have been used for θ and r. The number of Monte Carlo simulations is 500. The root mean square error (RMSE) $RMSE(\vartheta_k) = \sqrt{\frac{1}{KM_C}\sum_{k=1}^{K}(\widehat{\vartheta}_{qk} - \vartheta_k)^2}$, is adopted for quantitative evaluation, where $\widehat{\vartheta}_{qk}$ is the estimate of the parameter $\widehat{\theta}_k, \widehat{r}_k, \widehat{\gamma}_k, \widehat{\eta}_k$ in the qth Monte Carlo simulation, ϑ_k is the true value standing for the angle, range and polarization parameters, M_C is the number of Monte Carlo simulations and K is the number of signals.

In the first set of simulations, two near-field sources located at $(20^\circ, 2.5\lambda)$ and $(45^\circ, 2.7\lambda)$ impinge upon the array, whose corresponding polarization angles are $(55^\circ, 75^\circ)$ and polarization phase difference are $(100^\circ, 115^\circ)$. In the first test, the SNR is $0dB$ and the number of snapshot is 200. The number of COLDs in the x-direction satisfy $M = 2L + 1$. The RMSEs of the estimated DOA and range parameter versus the number of COLDs M are depicted in Fig. 2. It can be observed that the RMSEs of DOA and range param-

Please cite this article in press as: W. Wang et al., Quaternion-MUSIC for near-field strictly noncircular sources with large-scale polarization array, Digit. Signal Process. (2019), https://doi.org/10.1016/j.dsp.2019.06.005

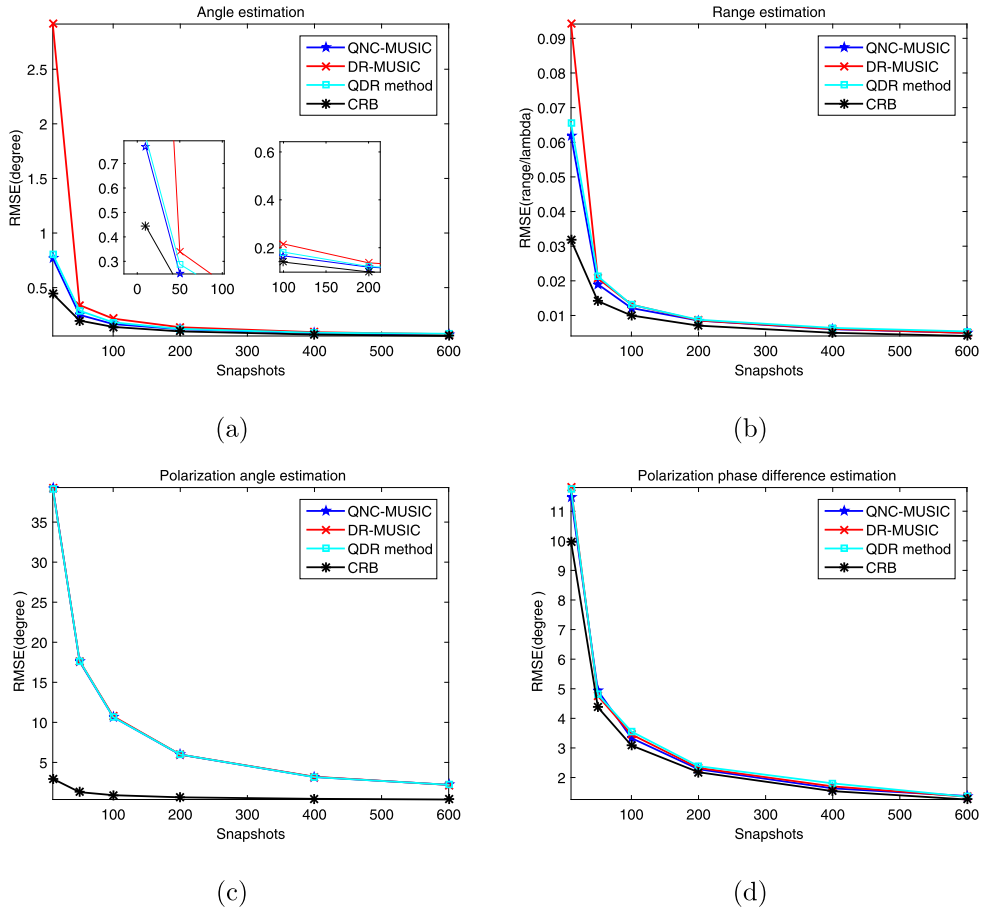

Fig. 4. RMSEs versus snapshot with SNR to be $-5dB$. (a) angle estimation. (b) range estimation. (c) polarization angle estimation. (d) polarization phase difference estimation.

eters of the two algorithms decrease as M increases. For the DOA and range estimation, the RMSEs of the QNC-MUSIC are smaller than those of the DR-MUSIC and approach the CRB closely. This is because that the quaternion model and the property of the non-circular signal have been used in the QNC-MUSIC to improve the accuracy of the DOA and range estimation.

In order to further show the performance of the proposed algorithm in massive MIMO systems, in the second and third set of simulations, we examine the performance of the proposed methods with above two near-field sources impinging upon a massive ULA with 65 CLODs.

In the second test, the snapshot number is $N = 100$. The RMSEs of the estimated DOA and polarization parameter versus the SNRs are depicted in Fig. 3. It can be observed that the RMSEs of these estimated parameters of the three algorithms decrease as SNR increases. For the DOA and range estimation, the RMSEs of the QNC-MUSIC is smaller than those of the DR-MUSIC and QDR method. The reason is identical with the first test. In addition, it can be seen from the experimental results that the performance advantage of QNC-MUSIC algorithm is more obvious when the SNR is low. Considering the application in real scene, the environment with low SNR is more common, so the advantages of the QNC-MUSIC algorithm will be more obvious.

In the third test, the SNR is $-5dB$. The RMSEs of the estimated DOA, range and polarization parameter versus the snapshot N received at the array are depicted in Fig. 4. It can be observed that the RMSEs of these estimated parameters of the three algorithms decrease as the snapshot number increases. For the DOA and range estimation, the RMSEs of the QNC-MUSIC is smaller than those of the DR-MUSIC and QDR method. The reason is identical with the first test. In addition, the curves shown in Fig. 4 become flat when the snapshot is higher than 200, which means that for the parameter estimation performance, the effect of the large snapshot is slightly less than that of the small snapshot. Considering the application in the real scene and the computational complexity, the performance of QNC-MUSIC algorithm in practical application scenarios should be better than that of DR-MUSIC algorithm. In massive MIMO systems, due to the increase of the number of array elements, the amount of calculation is multiplied. Reducing the number of snapshot is an important way to reduce the amount of calculation. Therefore, QNC-MUSIC algorithm is more suitable for massive MIMO systems.

From the results, we can see the proposed method outperform consistently the other methods for both DOA and range estimation. Particularly, when the SNR is low and the snapshot is small, the proposed method can also achieve an expected purpose. For QNC-MUSIC algorithm, the signal model is represented by quaternions, which could maintain the orthogonality of the magnetic and electric component and reduce the dimension of the data vector received by the array. At the same time, the non-circular information of the signals was exploited, which increased the array virtual aperture to some extent. Therefore, the performance of QNC-MUSIC algorithm is the best.

8. Conclusion

In this paper, we have proposed QNC-MUSIC algorithm, for the DOA, range and polarization estimation of the near-filed noncircular signals with a polarized array in massive MIMO systems. For the DOA and range estimation of noncircular signals using the QNC-MUSIC, the property of noncircular signals is used to further

Please cite this article in press as: W. Wang et al., Quaternion-MUSIC for near-field strictly noncircular sources with large-scale polarization array, Digit. Signal Process. (2019), https://doi.org/10.1016/j.dsp.2019.06.005

improve the DOA and range estimation accuracy. For the polarization estimation of the noncircular signal, the closed-form expression of the DR-MUSIC is adopted based on the DOA and range estimation result of the QNC-MUSIC. Compared with the traditional LV-MUSIC, the computational complexity of the QNC-MUSIC and the DR-MUSIC are much lower. Simulations show that the performance of the proposed QNC-MUSIC is better than DR-MUSIC and QDR method especially at low SNR and small snapshot.

Declaration of Competing Interest

We wish to draw the attention of the Editor to the following facts which may be considered as potential conflicts of interest and to significant financial contributions to this work.

We wish to confirm that there are no known conflicts of interest associated with this publication and there has been no significant financial support for this work that could have influenced its outcome.

We confirm that the manuscript has been read and approved by all named authors and that there are no other persons who satisfied the criteria for authorship but are not listed. We further confirm that the order of the authors listed in the manuscript has been approved by all of us.

We understand that the Corresponding Author is the sole contact for the Editorial process (including Editorial Manager and direct communication with the office). He is responsible for communicating with the other authors about the progress, submissions of revisions and final approval of proofs. We confirm that we have provided a current, correct email address which is accessible by Corresponding Author and which has been configured to accept email form the office.

Acknowledgments

This work was supported by Zhejiang Provincial Natural Science Foundation of China under Grant No. LQ19F010002, and by Natural Science Foundation of Ningbo Municipality under Grant No. 2018A610094, by National Natural Science Foundation of China under Grant No. 61801076 and 61571320.

References

[1] F. Rusek, D. Persson, B.K. Lau, E.G. Larsson, T.L. Marzetta, O. Edfors, F. Tufvesson, Scaling up MIMO: opportunities and challenges with very large arrays, IEEE Inst. Electr. Electron. Eng. 30 (1) (2013) 40–60.
[2] T.L. Marzetta, et al., Noncooperative cellular wireless with unlimited numbers of base station antennas, IEEE Trans. Wirel. Commun. 9 (11) (2010) 3590.
[3] T.L. Marzetta, E.G. Larsson, O. Edfors, F. Tufvesson, Massive MIMO for next generation wireless systems, IEEE Commun. Mag. 52 (2) (2014) 186–195.
[4] H. Yin, D. Gesbert, M. Filippou, Y. Liu, A coordinated approach to channel estimation in large-scale multiple-antenna systems, IEEE J. Sel. Areas Commun. 2 (31) (2013) 264–273.
[5] S. He, Y. Huang, H. Wang, S. Jin, L. Yang, Leakage-aware energy-efficient beamforming for heterogeneous multicell multiuser systems, IEEE J. Sel. Areas Commun. 32 (6) (2014) 1268–1281.
[6] R. Schmidt, Multiple emitter location and signal parameter estimation, IEEE Trans. Antennas Propag. 34 (3) (1986) 276–280.
[7] R. Roy, T. Kailath, ESPRIT-estimation of signal parameters via rotational invariance techniques, IEEE Trans. Acoust. Speech Signal Process. 37 (7) (1989) 984–995.
[8] J. Li, Y. Zhao, Channel characterization and modeling for large-scale antenna systems, in: 2014 14th International Symposium on Communications and Information Technologies, ISCIT, 2014, pp. 559–563.
[9] A. Manikas, J.W. Ng, Crossed-dipole arrays for asynchronous DS-CDMA systems, IEEE Trans. Antennas Propag. 52 (1) (2004) 122–131.
[10] C. Zhou, Y. Gu, Y.D. Zhang, Z. Shi, T. Jin, X. Wu, Compressive sensing-based coprime array direction-of-arrival estimation, IET Commun. 11 (11) (2017) 1719–1724.
[11] C. Zhou, Z. Shi, Y. Gu, X. Shen, DECOM: Doa estimation with combined music for coprime array, in: 2013 International Conference on Wireless Communications and Signal Processing, IEEE, 2013, pp. 1–5.
[12] Z. Shi, C. Zhou, Y. Gu, N.A. Goodman, F. Qu, Source estimation using coprime array: a sparse reconstruction perspective, IEEE Sens. J. 17 (3) (2017) 755–765.
[13] Y. Wu, H.C. So, C. Hou, J. Li, Passive localization of near-field sources with a polarization sensitive array, IEEE Trans. Antennas Propag. 55 (8) (2007) 2402–2408.
[14] J. He, M.O. Ahmad, M. Swamy, Near-field localization of partially polarized sources with a cross-dipole array, IEEE Trans. Aerosp. Electron. Syst. 49 (2) (2013) 857–870.
[15] S. Miron, N. Le Bihan, J.I. Mars, Quaternion-MUSIC for vector-sensor array processing, IEEE Trans. Signal Process. 54 (4) (2006) 1218–1229.
[16] N. Le Bihan, S. Miron, J.I. Mars, MUSIC algorithm for vector-sensors array using biquaternions, IEEE Trans. Signal Process. 55 (9) (2007) 4523–4533.
[17] X. Gong, Y. Xu, Z. Liu, Quaternion ESPRIT for direction finding with a polarization sensitive array, in: Signal Processing, 2008. ICSP 2008. 9th International Conference on, IEEE, 2008, pp. 378–381.
[18] B. Picinbono, P. Chevalier, Widely linear estimation with complex data, IEEE Trans. Signal Process. 43 (1995) 2030–2033.
[19] B. Picinbono, Second-order complex random vectors and normal distributions, IEEE Trans. Signal Process. 44 (10) (1996) 2637–2640.
[20] P. Gounon, C. Adnet, J. Galy, Localization angulaire de signaux non circulaires, Trait. Signal 15 (1) (1998) 17–23.
[21] C. Zhou, Y. Gu, X. Fan, Z. Shi, G. Mao, Y.D. Zhang, Direction-of-arrival estimation for coprime array via virtual array interpolation, IEEE Trans. Signal Process.
[22] C. Zhou, Y. Gu, S. He, Z. Shi, A robust and efficient algorithm for coprime array adaptive beamforming, IEEE Trans. Veh. Technol. 67 (2) (2018) 1099–1112.
[23] C. Zhou, Y. Gu, Z. Shi, Y.D. Zhang, Off-grid direction-of-arrival estimation using coprime array interpolation, IEEE Signal Process. Lett. 25 (11) (2018) 1710–1714.
[24] H. Chen, W. Liu, W.-P. Zhu, M. Swamy, Q. Wang, Mixed rectilinear sources localization under unknown mutual coupling, J. Franklin Inst. 356 (2019) 2372–2394.
[25] Y. Wang, L. Wang, J. Xie, M. Trinkle, B.W.-H. Ng, DOA estimation under mutual coupling of uniform linear arrays using sparse reconstruction, IEEE Wirel. Commun. Lett. (2019), https://doi.org/10.1109/LWC.2019.2903497.
[26] H. Chen, C. Hou, W.-P. Zhu, W. Liu, Y.-Y. Dong, Z. Peng, Q. Wang, ESPRIT-like two-dimensional direction finding for mixed circular and strictly noncircular sources based on joint diagonalization, Signal Process. 141 (2017) 48–56.
[27] H. Chen, C. Hou, W. Liu, W.-P. Zhu, M. Swamy, Efficient two-dimensional direction-of-arrival estimation for a mixture of circular and noncircular sources, IEEE Sens. J. 16 (8) (2016) 2527–2536.
[28] W.R. Hamilton, Theory of quaternions, in: Proceedings of the Royal Irish Academy (1836-1869), vol. 3, 1844, pp. 1–16.
[29] J. Ward, Quaternions and Cayley Numbers: Algebra and Applications, Mathematics and Its Applications, vol. 403, Kluwer, Dordrecht, 1997.
[30] N. Le Bihan, J. Mars, Singular value decomposition of quaternion matrices: a new tool for vector-sensor signal processing, Signal Process. 84 (7) (2004) 1177–1199.
[31] F. Zhang, Quaternions and matrices of quaternions, Linear Algebra Appl. 251 (1997) 21–57.
[32] J. He, M. Swamy, M.O. Ahmad, Efficient application of MUSIC algorithm under the coexistence of far-field and near-field sources, IEEE Trans. Signal Process. 60 (4) (2012) 2066–2070.
[33] K.T. Wong, M.D. Zoltowski, Uni-vector-sensor ESPRIT for multisource azimuth, elevation, and polarization estimation, IEEE Trans. Antennas Propag. 45 (10) (1997) 1467–1474.
[34] J. Si, T. Zhu, M. Zhang, Dimension-reduction MUSIC for jointly estimating DOA and polarization using plane polarized arrays, J. Commun. 35 (12) (2014) 28–35.
[35] H. Abeida, J.-P. Delmas, MUSIC-like estimation of direction of arrival for noncircular sources, IEEE Trans. Signal Process. 54 (7) (2006) 2678–2690.
[36] L. Wang, Z. Chen, G. Wang, Direction finding and positioning algorithm with COLD-ULA based on quaternion theory, J. Commun. 9 (2014) 778–784.
[37] H. Chen, W. Wang, W. Liu, Joint DOA, range, and polarization estimation for rectilinear sources with polarization sensitive array, IEEE Wirel. Commun. Lett. (2019), https://doi.org/10.1109/LWC.2019.2919542.
[38] F. Wen, X. Zhang, Z. Zhang, CRBs for direction-of-departure and direction-of-arrival estimation in collocated MIMO radar in the presence of unknown spatially coloured noise, IET Radar Sonar Navig. 13 (4) (2019) 530–537.
[39] H. Chen, W. Zhu, W. Liu, M. Swamy, Y. Li, Q. Wang, Z. Peng, RARE-based localization for mixed near-field and far-field rectilinear sources, Digit. Signal Process. 85 (2019) 54–61, https://doi.org/10.1016/j.dsp.2018.11.006.

Weifeng Wang was born in Hebei, China, on 1993. He received the bachelor degree in the College of Astronautics, Nanjing University of Aeronautics and Astronautics, Nanjing, China, in 2017. He is presently studying for a master's degree in Tianjin University, Tianjin, China. His current research interests include array signal processing and deep learning.

Hua Chen received the M.Eng. degree and Ph.D. degree in Information and Communication Engineering from Tianjin University, Tianjin, China, in

2013 and 2017, respectively. He is now as a lecturer in Faculty of Information Science and Engineering, Ningbo University, China. His research interests include array signal processing, MIMO radar and passive radar.

Jie Jin was born in China, on 1962. She received the bachelor's degree in electronic measurement and instrumentation, Department of electronic engineering, Tianjin University, Tianjin, China, in 1984 and master's degree in electromagnetic and microwave technology from the Department of electronic engineering, Tianjin University, Tianjin, China, in 1987. She received Ph.D. degree in optical instrument from Tianjin University, School of precision instrument and optoelectronics. Tianjin, China, in 1998. From 1998 to 2000, she entered the Mobile post-doctoral stations of condensed matter physics at Nankai University School of physics. She is presently a professor working in Tianjin University since she had worked in Hebei University of Technology from 1987 to 2001. Her research interests include: microwave device, microwave antenna design, fiber communication and device, solid laser and external cavity semiconductor laser, intelligent instrument and photoelectric technology. She has published more than 50 papers.

Xianpeng Wang was born in 1986. He received the M.S. and Ph.D. degrees from the College of Automation, Harbin Engineering University (HEU), Harbin, China, in 2012 and 2015, respectively. He was a full-time Research Fellow with the School of Electrical and Electronic Engineering, Nanyang Technological University, Singapore, from 2015 to 2016. He is currently a Professor with the College of Information and Communication Engineering, Hainan University. He is the author of over 60 papers published in related journals and international conference proceedings. His major research interests include communication systems, array signal processing, radar signal processing, and compressed sensing and its applications. He has served as a Reviewer for over 20 journals.

Liangtian Wan received the B.S. degree and the Ph.D. degree in the College of Information and Communication Engineering from Harbin Engineering University, Harbin, China, in 2011 and 2015, respectively. From Oct. 2015 to Apr. 2017, he has been a Research Fellow of School of Electrical and Electrical Engineering, Nanyang Technological University, Singapore. He is currently an Associate Professor of School of Software, Dalian University of Technology, China. He is the author of over 30 articles published in related international conference proceedings and journals. Dr. Wan has been serving as an Associate Editor for IEEE Access and Journal of Information Processing Systems. His current research interests include social network analysis and mining, big data, array signal processing, wireless sensor networks, compressive sensing.

Xiaowei Zhang received his Ph.D. degree from School of Electronic Science and Engineering, Nanjing University in 2016, following the two-year Joint PhD Student Program at University of California at Berkeley. Now, he is an associate professor in School of Electrical Engineering and Computer Science, Ningbo University. His current research interests focus on design and fabrication of novel semiconductor devices and array signal processing.

Please cite this article in press as: W. Wang et al., Quaternion-MUSIC for near-field strictly noncircular sources with large-scale polarization array, Digit. Signal Process. (2019), https://doi.org/10.1016/j.dsp.2019.06.005